ELSEVIER

Full paper / Mémoire

Interplay of metallic and ionic bonding in layered subnitrides AE_2N (AE = Ca, Sr, or Ba) under high pressure

Grigori V. Vajenine [a,*], Andrzej Grzechnik [a,1], Karl Syassen [a], Ingo Loa [a], Michael Hanfland [b], Arndt Simon [a]

[a] *Max-Planck-Institut für Festkörperforschung, Heisenbergstr. 1, 70569 Stuttgart, Germany*
[b] *European Synchrotron Radiation Facility, BP 220, 38043 Grenoble, France*

Abstract

Layered alkaline earth-metal subnitrides AE_2N (AE = Ca, Sr, or Ba) adopting the *anti*-CdCl$_2$-type structure (space group $R\bar{3}m$) were structurally investigated under pressures up to 40 GPa using diamond-anvil cells for pressure application and synchrotron radiation for collecting powder diffraction patterns. Anisotropic compressibility and structural changes under pressure were found to be consistent with the spatial separation of ionic and metallic bonding according to the formal description as $(AE^{2+})_2N^{3-} \bullet e^-$. Further increase of pressure was found to induce several phase transitions: in the case of Ba$_2$N, in addition to a new layered *anti*-CdI$_2$-type modification (space group $P\bar{3}m1$), a cubic *anti*-Th$_3$P$_4$-type structure ($I\bar{4}3d$), and its distorted analogue were identified. The latter appears to be isostructural to the observed high-pressure phases of Ca$_2$N and Sr$_2$N. ***To cite this article: G.V. Vajenine et al., C. R. Chimie 8 (2005)***.

© 2005 Académie des sciences. Published by Elsevier SAS. All rights reserved.

Résumé

La structure des nitrures d'alcalino-terreux en couche AE_2N (AE = Ca, Sr, ou Ba) cristallisant dans l'antitype de CdCl$_2$ (groupe d'espace $R\bar{3}m$) a été étudiés pour des pressions allant jusqu'à 40 GPa, en utilisant une cellule diamant pour la pression appliquée et un rayonnement synchrotron pour la collecte des clichés de diffraction sur poudre. Une compressibilité anisotropique ainsi que des changements structuraux ont été mis en évidence de manière compatible avec la séparation spaciale de la liaison ionique et métallique, en accord avec la description formelle $(AE^{2+})_2N^{3-} \bullet e^-$. Une augmentation plus ample de la pression a permis de mettre en évidence plusieurs transitions de phase: dans le cas de Ba$_2$N, en plus d'une modification vers la nouvelle structure en feuillet anti-type de CdI$_2$ (groupe d'espace $P\bar{3}m1$), une structure cubique anti-type de Th$_3$P$_4$ ($I\bar{4}3d$) ainsi que ses variantes desordonnées ont été identifiées. Ce dernier semble être isostructural aux phases hautes pressions observées pour Ca$_2$N et Sr$_2$N. ***Pour citer cet article : G.V. Vajenine et al., C. R. Chimie 8 (2005)***.

© 2005 Académie des sciences. Published by Elsevier SAS. All rights reserved.

---

* Corresponding author.

E-mail address: G.Vajenine@fkf.mpg.de (G.V. Vajenine).

[1] Present address: Universidad del País Vasco, Facultad de Ciencias, Departamento de Fisica de la Materia Condensada, Apartado 644, 48080 Bilbao, Spain.

1. Introduction

Binary alkaline earth (*AE*) subnitrides AE_2N (*AE* = Ca [1,2], Sr [3], or Ba [4]) feature a rather unique combination of ionic and metallic bonding within the same crystal structure. If one attempts to assign the typical oxidation states to the elements involved (AE^{2+} and N^{3-}), one valence electron per formula unit is left over due to the requirement of the overall charge neutrality, leading to the formal description $(AE^{2+})_2N^{3-} \bullet e^-$. The crystal structure of the three binary subnitrides (space group $R\bar{3}m$ with $Z = 3$ in hexagonal setting, *anti*-CdCl$_2$ structure type) is built from two-dimensional hexagonal double layers of *AE* metal atoms, with nitrogen atoms centering AE_6 octahedra within the layers (Fig. 1). One would expect that the remaining valence electrons avoid the space around the formally trivalent nitride anions due to electrostatic repulsion and are thus expelled into the *inter*-layer region. A spatial separation of ionic and metallic bonding is the result: while ionic bonding between AE^{2+} and N^{3-} holds the AE_2N layers together, metallic *inter*-layer bonding is due to

the nearly free remaining electrons, much like in metals themselves.

Such a bonding description, termed *void metal* [5], has been also postulated for the related alkali metal suboxides and other alkaline earth metal subnitrides, such as $Cs_{11}O_3$ and $NaBa_3N$, for example. This viewpoint has been supported by resistivity and photoelectron spectroscopy measurements on alkali metal suboxides [6,7] and by TB-LMTO band structure calculations on $NaBa_3N$ [8]. Chemical arguments, such as bonding distances, atomic thermal displacement factors, and crystal volume considerations, also speak for the spatial separation of the two kinds of bonding in the crystal structures of suboxides and subnitrides [5,6,9]. Moreover, electrostatic repulsion between the respective anions (O^{2-} or N^{3-}) and the remaining valence electrons leads to a lowering of the work function, as observed in the case of $Cs_{11}O_3$ [7], for instance.

The interplay of ionic and metallic bonding in such compounds can be investigated further by carrying out a structural study at high-pressure: while the relatively compressible metallic regions of the respective crystal structures are expected to deform significantly under pressure, the rigid ionic regions should be much less affected by pressure. Layered AE_2N subnitrides are a good test subject for such a study, as the expected anisotropy in compressibility would be apparent from the change in lattice constants under pressure, while structure refinement of the collected data would shed light on the relative compressibility of the ionic and metallic regions. Here we report the results of high-pressure powder diffraction studies, which were carried out with diamond-anvil cells (DACs) using synchrotron radiation.

2. Experimental

AE_2N samples were prepared from the elements, with special attention paid to avoiding impurities such as hydrogen and oxygen: the metals were sublimed in vacuum twice and all sample handling was carried out under an atmosphere of purified argon [10]. No pres-
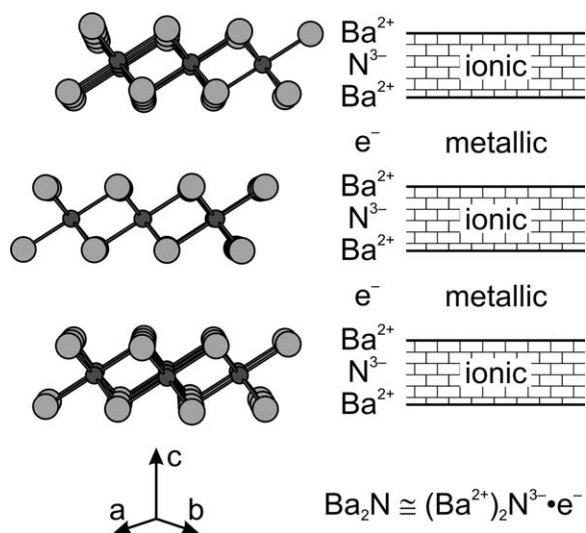

Fig. 1. Crystal structure of Ba$_2$N (left, space group $R\bar{3}m$ in hexagonal setting, *anti*-CdCl$_2$ structure type) and formal description of chemical bonding (right). Ca$_2$N and Sr$_2$N are isostructural to Ba$_2$N.

sure medium was used when loading samples into DACs because of the high reactivity of the subnitrides. The ruby luminescence method was used for pressure measurement [11,12]. In some samples Ta powder was included as a pressure standard [13]. The Ca_2N, Sr_2N, and Ba_2N samples were investigated at pressures up to 14, 30, and 40 GPa, respectively. Angle-dispersive powder X-ray diffraction patterns were measured at room temperature at the ID09 beam line of the European Synchrotron Radiation Facility in Grenoble. Monochromatic radiation with a wavelength of 0.417 Å was used for pattern collection on an image plate detector. Integration of two-dimensional images was carried out using the program FIT2D [14] yielding intensity vs. 2θ diagrams. Powder averaging was improved by rotating the DACs. Some samples were annealed at 200 °C for several hours after applying pressure, but this treatment did not significantly improve the quality of the collected diffraction patterns.

Full Rietveld refinement of the collected X-ray diagrams was carried out using the GSAS program [15]. The refined parameters were the hexagonal unit cell constants a and c, the fractional coordinate z of the alkaline earth metal atoms, isotropic thermal displacement parameters for the *AE* atoms (with U_{iso} for nitrogen fixed at 0.02 Å^2), Chebyschev polynomial background, a profile function employing the microstrain broadening description of Stephens [16], a spherical harmonic preferred orientation correction necessary due to the layered nature of the compounds, phase fractions, and an overall intensity scaling factor. The Stephens function was used in order to take into account the effects of nonhydrostaticity due to the absence of a pressure medium. Further details of the crystal structure investigations may be obtained from the Fachinformationszentrum Karlsruhe, 76344 Eggenstein-Leopoldshafen, Germany, on quoting the depository numbers CSD-414329 (Ca_2N-I), CSD-414330 (Sr_2N-I), and CSD-414328 (Ba_2N-I and Ba_2N-II).

3. Results and discussion

3.1. General behavior under high pressure

The evolution of the integrated powder diffraction diagrams with increasing pressure is shown in Figs. 2–4. In the case of calcium and strontium subnitrides,
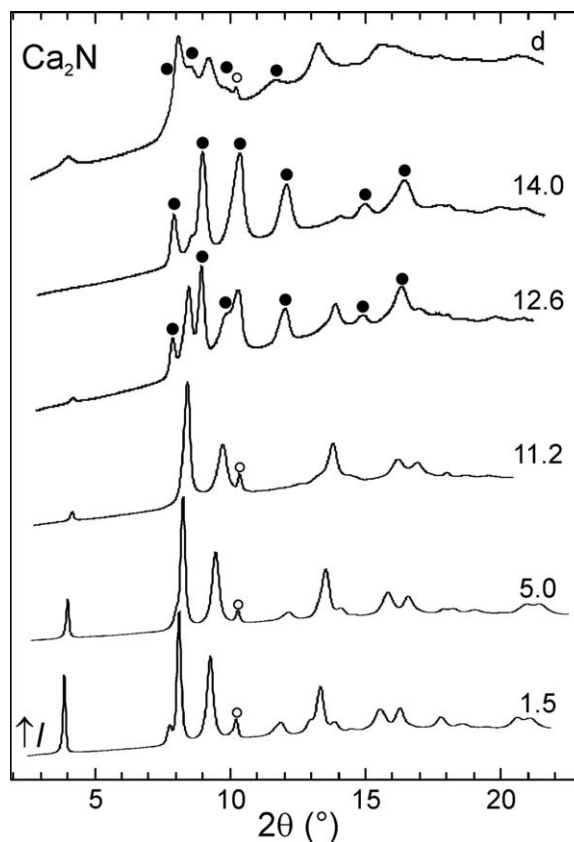

Fig. 2. Selected powder diffraction diagrams for Ca_2N. The sample pressure is given in GPa next to each pattern. The uppermost diagram was measured upon decompression. Reflections corresponding to the high-pressure Ca_2N-II phase (●) and to the Ta standard (○) are marked.

pressure-induced phase transitions Ca_2N-I→Ca_2N-II and Sr_2N-I→Sr_2N-II were observed around 12 GPa. These phase transitions are reversible and the starting Ca_2N-I and Sr_2N-I phases were almost fully recovered upon decompression. Three pressure-induced phase transitions took place in the case of Ba_2N. First, Ba_2N-I transformed into Ba_2N-II at 2 GPa. The next high-pressure phase, Ba_2N-III, was observed only in a narrow pressure window around 7 GPa, followed by Ba_2N-IV. The latter phase was also the major component observed after decompressing the sample, accompanied by a small amount of Ba_2N-II.

The crystal structure of Ba_2N-II is closely related to that of the starting phase (Ba_2N-I): both consist of 2D-Ba_2N layers, but the stacking of these layers is different. While the *anti*-$CdCl_2$-type structure (Ba_2N-I) is stable at ambient pressure, the alternative *anti*-CdI_2
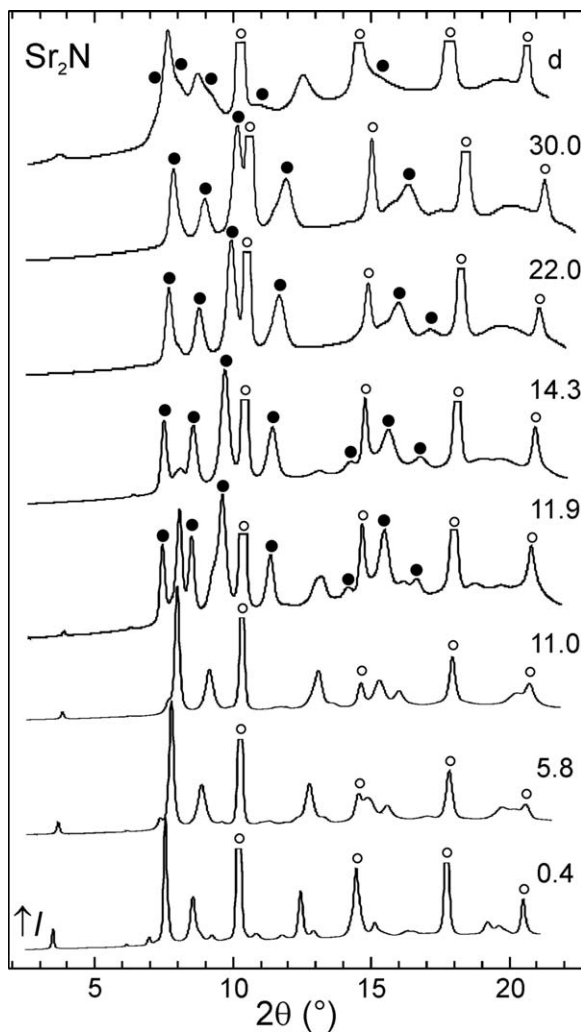
Fig. 3. Selected powder diffraction diagrams for Sr_2N. The sample pressure is given in GPa next to each pattern. The uppermost diagram was measured upon decompression. Reflections corresponding to the high-pressure Sr_2N-II phase (●) and to the Ta standard (○) are marked.

structure type ($P\bar{3}m1$, $Z = 1$) is adopted by the Ba_2N-II phase. Only a small volume decrease of 1.6% accompanies this transition. It has already been suggested [17], that stacking faults might play a role in the structural chemistry of the EA_2N subnitrides, leading to a range of the observed values for the c lattice constant depending on the preparation conditions, for example. The existence of two energetically close ways to stack the 2D-Ba_2N layers would support this suggestion. Since the qualitative bonding picture and dimensionality are
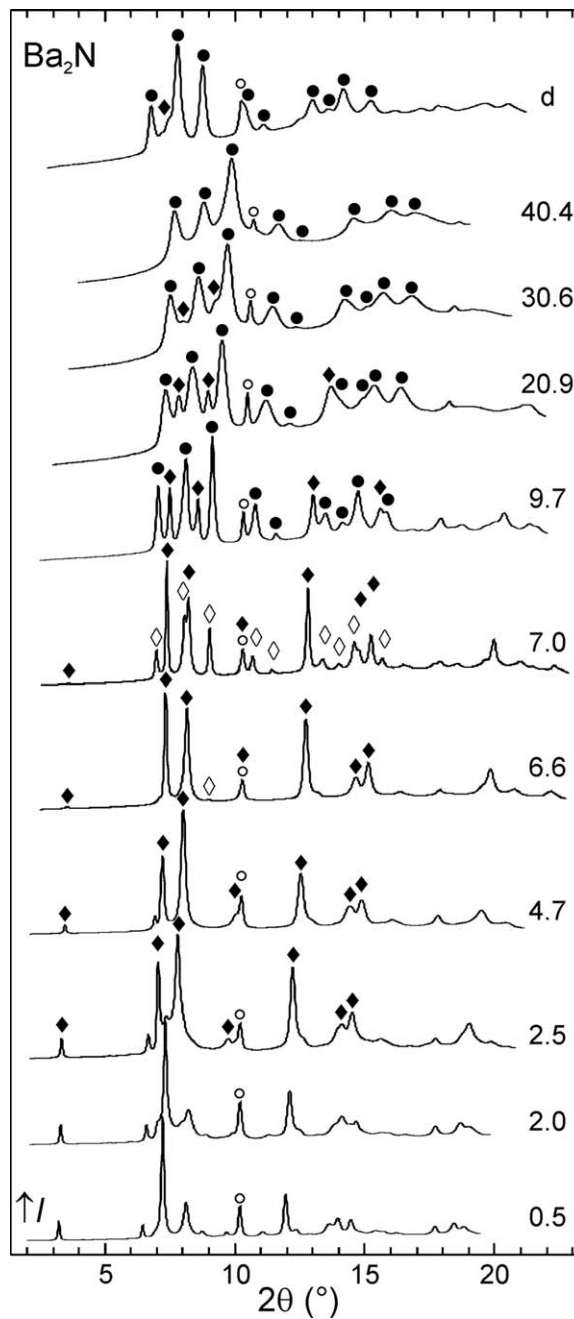

Fig. 4. Selected powder diffraction diagrams for Ba_2N. The sample pressure is given in GPa next to each pattern. The uppermost diagram was measured upon decompression. Reflections corresponding to the high-pressure Ba_2N-II (♦), Ba_2N-III (◇), and Ba_2N-IV (●) phases and to the Ta standard (○) are marked.

preserved in this transition, we will consider Ba_2N-II together with the AE_2N-I phases in the following.

Full structural characterization of the high-pressure Ba_2N-III, Ba_2N-IV, Ca_2N-II, and Sr_2N-II phases was not possible based on the available diffraction data. The cubic Ba_2N-III, stable only around 7 GPa, appears to have a crystal structure which is completely different from those of the layered phases. The last observed high-pressure barium subnitride phase, Ba_2N-IV, as well as Ca_2N-II and Sr_2N-II, is likely to be a distorted variant of the cubic Ba_2N-III phase. These phases will be addressed in more detail below.

3.2. Compressibility of the layered subnitrides

The collected powder diffraction patterns for the layered phases Ca_2N-I, Sr_2N-I, Ba_2N-I, and Ba_2N-II, were used to refine the unit cell parameters of the respective structures as a function of pressure. The unit cell volume per formula unit (V/Z) for the four layered structures as a function of pressure is shown in Figs. 5–7. The $V(P)$ data were fitted using the Birch equation of state [18] in order to extract the values (all at zero pressure) of the unit cell volume (V_0), bulk modulus (B_0), and the first derivative of the bulk modulus (B'_0). These fits resulted in the following bulk modulus values (B_0): 45(4) GPa for Ca_2N-I, 33(3) GPa for Sr_2N-I, and 21(6) GPa for the two layered Ba_2N phases. For comparison, the values of the bulk modulus for the respec-

Fig. 6. Crystal volume per formula unit as a function of pressure for Sr_2N.

tive metals are 17.4(1) GPa (Ca), 11.88(5) GPa (Sr), and 8.93(6) GPa (Ba) [19]. No high-pressure experimental data on the closed-shell AE_3N_2 nitrides exists. Only the recently reported theoretical B_0 value of 70.1 GPa for Ca_3N_2 [20] can be taken as a reference. The experimentally measured B_0 values for the ionic oxides CaO (114(9) GPa [21]), SrO (88(7) GPa [21]), and BaO (74.0(2) GPa [22]) are somewhat higher. Thus the alkaline earth metal subnitrides lie between the pure metals and the related ionic compounds as far as compressibility is concerned.
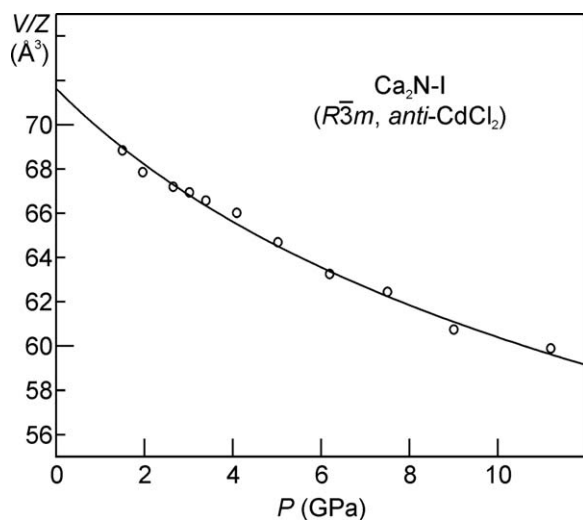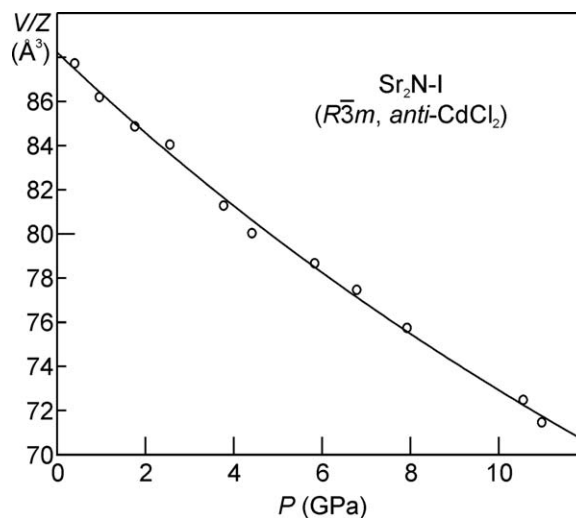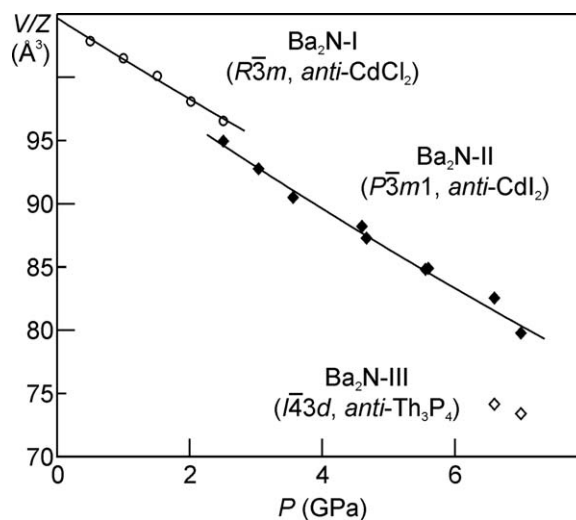

Fig. 5. Crystal volume per formula unit as a function of pressure for Ca_2N.

Fig. 7. Crystal volume per formula unit as a function of pressure for Ba_2N.

Anisotropic compressibility of the Ca_2N-I, Sr_2N-I, Ba_2N-I, and Ba_2N-II phases is another consequence of the layered structure. Fig. 8 shows the c/a ratio for these structures as a function of pressure. Typical for layered compounds, compressibility is larger perpendicular to the layers than in the plane of the layers, resulting in a reduction of the c/a ratio with increasing pressure. The compressibility along the c-axis was found to be about twice as large as that along the a-axis for all four phases.

In order to find out, whether the metallically or the ionically bonded regions of the layered subnitride phases are more compressible, Rietveld refinement of the respective crystal structures was carried out based on the diffraction patterns collected under pressure. The evolution of the only free atomic parameter (z of the AE metal atoms) as a function of pressure is shown in Fig. 9. Decreasing value of $z(AE)$ with increasing pressure is a sign that the metallic gap between the AE_2N layers is closing. In other words, the metallically bonded regions are more compressible than the ionically bonded ones. Structural details for the layered subnitrides are summarized in Table 1.

3.3. Beyond the layered structures

Increase of the pressure applied to the layered subnitrides leads to phase transitions in which the 2D structural features are lost. In the case of Ba_2N, a new Ba_2N-
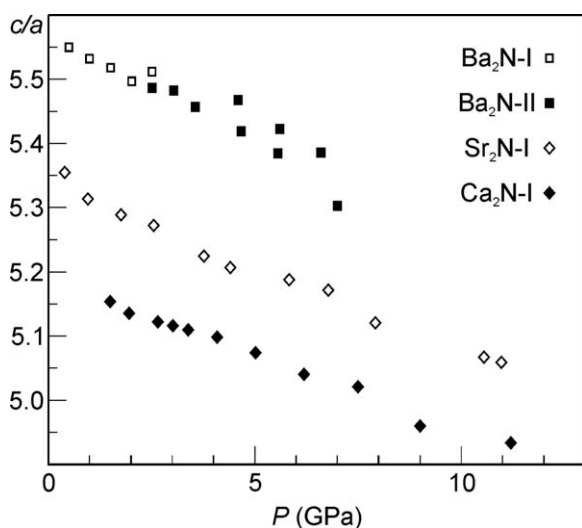

Fig. 8. The c/a ratio for the layered AE_2N phases as a function of pressure. The values for the Ba_2N-II phase were tripled in order to allow for a comparison. A closest packing of spheres (AE metal atoms) corresponds to the c/a value of $2\sqrt{6} = 4.899$.
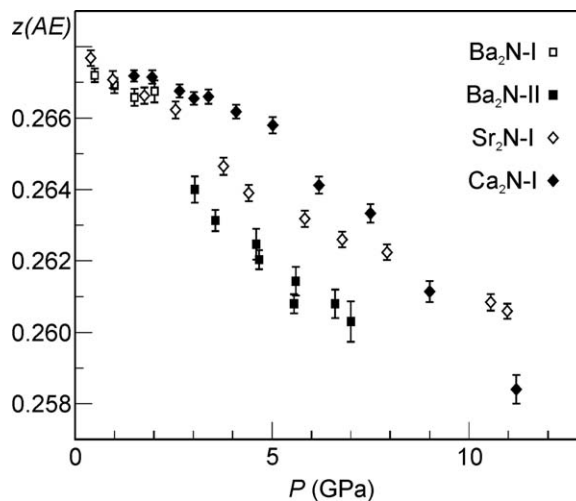

Fig. 9. The z parameter of the AE metal atoms in the layered subnitrides as a function of pressure. The values for the Ba_2N-II phase were converted according to $(1 – z)/3$ in order to allow for a comparison. A closest packing of spheres (AE metal atoms) corresponds to the $z(AE)$ value of 0.25. For example, $z = 0.2520$ in $CdCl_2$ [30] and $(1 – z)/3 = 0.2503$ in CdI_2 [31].

III phase follows the layered Ba_2N-II phase at 7 GPa. The strongest peaks of this phase could be indexed with a cubic body-centered unit cell (see also Fig. 4). Based on the observed reflection conditions the space group $I\bar{4}3d$ (220) was chosen. The observed relative intensities were consistent with a crystal structure containing barium atoms in the $16c$ position (x, x, x).

Although this cubic phase is stable only in a narrow pressure window around 7 GPa and could therefore not be observed in a pure form, it was possible to carry out a Rietveld refinement of data collected on a Ba_2N sample containing ca. 40% Ba_2N-III and 60% Ba_2N-II (see Fig. 10). The refined barium position with $x = 0.0480(3)$ corresponds to the phosphorus substructure of Th_3P_4. The a-axis was found to be 8.3741(5) Å; refinement of the isotropic thermal displacement parameter for Ba resulted in a reasonable value of 0.026(2) Å^2 for U_{iso}.

The space group $I\bar{4}3d$ does not have an eightfold position which would be suitable for the nitrogen atoms. Insertion of N atoms in the $12a$ (3/8, 0, 1/4) site (Th position in Th_3P_4) with the occupancy of 2/3 in order to satisfy the overall stoichiometry causes little change in the refinement results, as one might expect due to the large difference between the barium and nitrogen atoms in terms of the scattering factors.

Table 1
Structural details for the layered alkaline earth-metal subnitrides

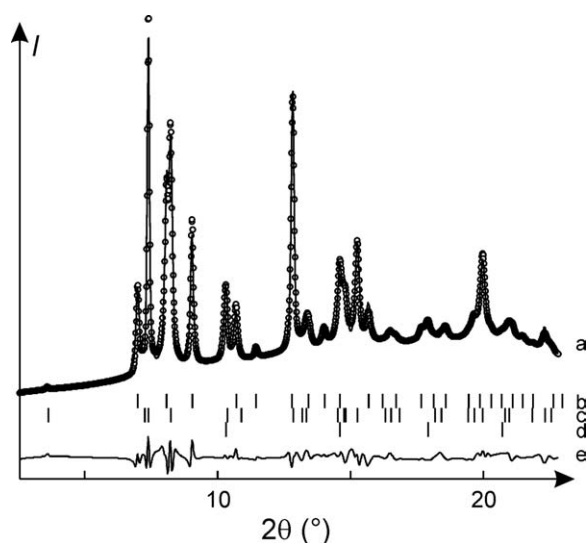| Phase	P (GPa)	Space group, Z	a (Å)	c (Å)	AE position	N position
Ca_2N-I	4.1	$R\bar{3}m$, 3	3.5530(3)	18.114(3)	6c (0, 0, 0.2662(2))	3a (0, 0, 0)
Sr_2N-I	4.4	$R\bar{3}m$, 3	3.7622(3)	19.589(8)	6c (0, 0, 0.2639(2))	3a (0, 0, 0)
Ba_2N-I	1.0	$R\bar{3}m$, 3	3.9908(3)	22.079(7)	6c (0, 0, 0.2669(2))	3a (0, 0, 0)
Ba_2N-II	4.7	$P\bar{3}m1$, 1	3.8211(3)	6.902(2)	2d (1/3, 2/3, 0.2138(8))	1a (0, 0, 0)

Fig. 10. Rietveld refinement of powder diffraction data collected on a Ba_2N sample at 7 GPa. The measured points are shown with circles, the fit is given by a solid line (**a**). The positions of the reflections for the phases involved are marked with tics (**b**: cubic Ba_2N-III; **c**: layered Ba_2N-II; **d**: Ta standard). The difference between the measured and calculated patterns is shown at the bottom (**e**).

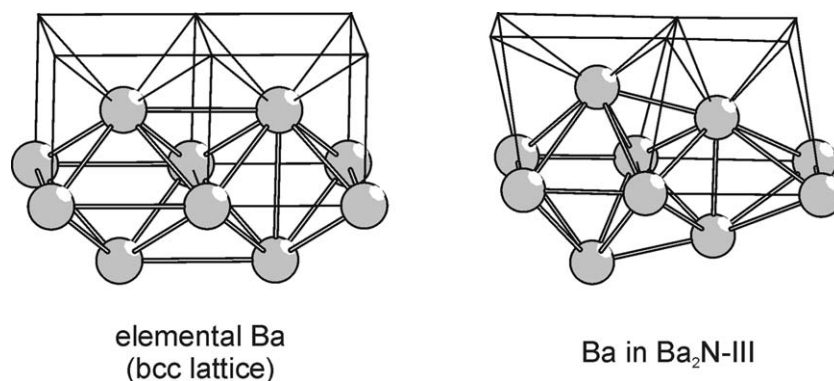The Ba-substructure of Ba_2N-III is best described by a body-centered cubic (*bcc*) lattice with the unit cell doubled in all three directions and with all atoms slightly displaced from their positions along the body diagonals while maintaining the overall cubic symmetry. That is, setting the value of x to zero would return the Ba-array of Ba_2N-III back to the ideal *bcc* arrangement as found in elemental barium at ambient conditions (see Fig. 11). The Ba-substructure of Ba_2N-III can also be described as a space-filling arrangement of tetrahedra and bisdisphenoids (trigon-dodecahedra). The 12a sites lie exactly in the centers of these bisdisphenoids. If these positions were to be occupied by the nitrogen atoms, the coordination number of the latter would increase from six in the layered subnitrides to eight. Assuming this crystal structure for Ba_2N-III, a crystal volume decrease of 8% accompanies the Ba_2N-II→Ba_2N-III phase transition.

Although we are not aware of other examples of Th_3P_4-type structures with a partial occupation of the Th-site, there are quite a few reports on A_2BX_4 compounds with A and B atoms taking this position. While in some cases no deviation from the cubic symmetry was observed (as in an anti-type Rb_4Cl_2O [23], see also references therein), ordering of the different atoms occupying the Th-position can lead to a lowering of symmetry as in $K_2M^{II}Cl_4$ (M^{II} = Sr, Ba, Eu, or Pb), for example [24,25].

elemental Ba
(bcc lattice)

Ba in Ba_2N-III

Fig. 11. Distortion of a bcc arrangement of Ba atoms leading to the Ba-substructure of the cubic Ba_2N-III phase. Thick lines represent the edges of the resulting tetrahedra and bisdisphenoids, while the thin lines track the bcc lattice.

The partial occupation of the 12*a* position by the nitrogen atoms might be the reason for a relatively low structural stability of the cubic Ba_2N-III phase, which exists in a narrow pressure window. One might expect, that still higher pressure induces an ordering of the N atoms in two thirds of the available bisdisphenoids, leading to a less symmetrical structure. Indeed, such a distortion apparently takes place and a new phase, Ba_2N-IV, results. Although the details of its structure are still unknown, the overall shape of its powder diffraction pattern resembles that of the cubic Ba_2N-III with clear signs of a distortion, such as splitting of the existing and appearance of new peaks. Interestingly, in the cases of Ca_2N and Sr_2N direct transitions from the *anti*-CdCl$_2$-type structures (Ca_2N-I and Sr_2N-I) to the distorted *anti*-Th$_3$P$_4$-type structures (Ca_2N-II and Sr_2N-II) take place. The analogy between the latter two structures and the Ba_2N-IV phase can be assumed based on the similarities between their powder diffraction patterns (compare Figs. 2–4).

It is remarkable that a cubic *cI*16 (the Ba-substructure of Ba_2N-III) structure was recently observed in high-pressure studies on elemental Li [26]. This cubic phase was found to be superconducting with T_c between 10 and 20 K according to different reports [27–29].

4. Conclusions

The high-pressure behavior of the layered AE_2N (AE = Ca, Sr, or Ba) subnitrides was investigated up to 40 GPa by means of powder X-ray diffraction using a synchrotron radiation source. A new layered modification of the barium subnitride, Ba_2N-II with the *anti*-CdI$_2$-type structure, was observed in the pressure range from 2 to 7 GPa. The observed bulk modulus values for the layered subnitrides are larger than those for the pure metals, but lower than those for the related ionic compounds. The compressibility along the *c*-axis was found to be about twice as high compared to that along the *a*-axis for all layered AE_2N phases, resulting in a decreasing *c*/*a* ratio with increasing pressure. The *z* parameter of the AE metal atoms was also found to decrease under pressure, indicating higher compressibility of the metallically bonded *inter*-layer region in the AE_2N structures. All of these findings are in agreement with the chemical bonding picture for these compounds according to the formal description $(AE^{2+})_2N^{3-}$ ·e^-. Further increase of pressure was found to induce phase transitions resulting in a cubic *anti*-Th$_3$P$_4$-type Ba_2N-III structure, related to a high-pressure modification of Li, and its distorted variants Ca_2N-II, Sr_2N-II, and Ba_2N-IV.

References

[1]   E.T. Keve, A.C. Skapski, Inorg. Chem. 7 (1968) 1757.
[2]   D.H. Gregory, A. Bowman, C.F. Baker, D.P. Weston, J. Mater. Chem. 10 (2000) 1635.
[3]   J. Gaudé, P. L'Haridon, Y. Laurent, J. Lang, Bull. Soc. Fr. Minéral Cristallogr. 95 (1972) 56.
[4]   S.M. Ariya, E.A. Prokofyeva, I.I. Matveeva, J. Gen. Chem. USSR Engl. Transl. 25 (1955) 609.
[5]   A. Simon, Coord. Chem. Rev. 163 (1997) 253.
[6]   A. Simon, Struct. Bond. 36 (1979) 81.
[7]   G. Ebbinghaus, A. Simon, Chem. Phys. 43 (1979) 117.
[8]   H. Weiss, G.V. Vajenine, U. Steinbrenner, A. Simon, E. Balthes, P. Wyder, Phys. Rev. B 63 (2001) 115104.
[9]   G.V. Vajenine, U. Steinbrenner, A. Simon, C. R. Acad. Sci. Paris, Ser. IIc 2 (1999) 583.
[10] U. Steinbrenner, PhD thesis, Stuttgart, 1997.
[11] G.J. Piermarini, S. Block, J.D. Barnett, R.A. Forman, J. Appl. Phys. 46 (1975) 2774.
[12] H.K. Mao, J. Xu, P.M. Bell, J. Geophys. Res. 91 (1986) 4673.
[13] M. Hanfland, K. Syassen, J. Köhler, J. Appl. Phys. 91 (2002) 4143.
[14] A.P. Hammersley, S.O. Svensson, M. Hanfland, A.N. Fitch, D. Häusermann, High-Pressure Res. 14 (1996) 235.
[15] A.C. Larson, R.B. von Dreele, GSAS: General Structure Analysis System, Los Alamos National Laboratory, 1996.
[16] P.W. Stephens, J. Appl. Crystallogr. 32 (1999) 281.
[17] O. Reckeweg, F.J. DiSalvo, Solid-State Sci. 4 (2002) 575.
[18] F. Birch, Phys. Rev. 71 (1947) 809.
[19] M.S. Anderson, C.A. Swenson, D.T. Peterson, Phys. Rev. B 41 (1990) 3329.
[20] A. Mokhtari, H. Akbarzadeh, Phys. B (Amsterdam) 337 (2003) 122.
[21] P.R. Son, R.A. Bartels, J. Phys. Chem. Solids 33 (1972) 819.
[22] K.-O. Park, J.M. Sivertsen, Phys. Lett. A 55 (1975) 62.

[23] A.-V. Mudring, M. Jansen, Z. Kristallogr, NCS 216 (2001) 483.

[24] H. Fink, H.-J. Seifert, Z. Anorg, Allg. Chem. 466 (1980) 87.

[25] H.-J. Seifert, J. Warczewski, K. Burhenn, Rev. Chim. Minér. 20 (1983) 504.

[26] M. Hanfland, K. Syassen, N.E. Christensen, D.L. Novikov, Nature 408 (2000) 174.

[27] V.V. Struzhkin, M.I. Eremets, W. Gan, H.-K. Mao, R.J. Hemley, Science 298 (2002) 1213.

[28] K. Shimizu, H. Ishikawa, D. Takao, T. Yagi, K. Amaya, Nature 419 (2002) 597.

[29] S. Deemyad, J.S. Schilling, Phys. Rev. Lett. 91 (2003) 167001.

[30] D.E. Partin, M. O'Keeffe, J. Solid-State Chem. 95 (1991) 176.

[31] B. Palosz, E. Salje, J. Appl. Crystallogr. 22 (1989) 622.